

# Modeling of Hybrid Wind-Photo Voltaic Energy Systems for Grid Connected Applications Based on Conventional and Fuzzy Logic Controllers

V. Prasanna<sup>1</sup>, N.PremaKumar<sup>2</sup>

<sup>1</sup>Department of Electrical Engineering, Andhra University, Visakhapatnam, India  
prasanna\_april14@yahoo.co.in

<sup>2</sup>Department of Electrical Engineering, Andhra University, Visakhapatnam, India  
prem\_navuri@yahoo.co.in

**Abstract:** This paper presents power-control strategies of a grid-connected hybrid generation system with versatile power transfer. The hybrid system allows maximum utilization of freely available renewable sources like wind and photovoltaic energies. This paper presents a new system configuration of the multi input rectifier stage for a hybrid wind and photovoltaic energy system. This configuration allows the two sources to supply the load simultaneously depending on the availability of the energy sources. The multi-input rectifier stage also allows Maximum Power Point Tracking (MPPT) to be used to extract maximum power from the sun when it is available. An adaptive MPPT algorithm with a standard perturb and observed method will be used for the Photo Voltaic system. The main advantage of the hybrid system is to give continuous power supply to the load. The gating pulses to the inverter switches are implemented with conventional and fuzzy controller. This hybrid wind-photo voltaic system is modeled in MATLAB/SIMULINK environment. Simulation circuit is analyzed and results are presented for this hybrid wind and solar energy system.

**Keywords:** CUK, Maximum Power Point Tracking (MPPT), Photovoltaic (PV) system, Voltage Source converter (VSC)

## 1. Introduction

With increasing concern of global warming and the depletion of fossil fuel reserves, many are looking at sustainable energy solutions to preserve the earth for the future generations. Other than hydro power, wind and photovoltaic energy holds the most potential to meet our energy demands. Alone, wind energy is capable of supplying large amounts of power but its presence is highly unpredictable as it can be here one moment and gone in another. Similarly, solar energy is present throughout the day but the solar irradiation levels vary due to sun intensity and unpredictable shadows cast by clouds, birds, trees, etc. The common inherent drawback of wind and photo voltaic systems are their intermittent natures that make them unreliable. However, by combining these two intermittent sources along and by incorporating maximum power point tracking (MPPT) algorithms, the system's power transfer efficiency and reliability can be improved significantly. When a source is unavailable or insufficient in meeting the load demands, the other energy source can compensate for the difference. Several hybrid wind/PV power systems with MPPT control have been proposed and discussed in works.

Most of the systems in literature use a separate DC/DC boost converter connected in parallel in the rectifier stage as shown in Figure 1 to perform the MPPT control for each of the renewable energy power sources. A simpler multi input structure has been suggested by that combine the sources from the DC-end while still achieving MPPT for PV renewable source. The structure is implemented by a cuk converter.

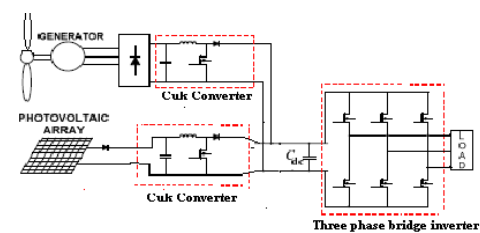


**Figure 1:** Hybrid system with multi-connected cuk converter

The systems in literature require passive input filters to remove the high frequency current harmonics injected into wind turbine generators. The harmonic content in the generator current decreases its lifespan and increases the power loss due to heating. In this project, an alternative multi-input rectifier structure is proposed for hybrid wind/solar energy systems. The system design is a fusion of the Cuk converters. The features of the system topology are:

- 1) The inherent nature of these cuk converters eliminates the need for separate Input filters for PFC.
  - 2) It can support step up/down operations for each renewable source (can support wide ranges of PV and wind input).
  - 3) MPPT can be realized for PV Source.
  - 4) Individual and simultaneous operation is supported.
- The circuit operating principles will be discussed in this project. Simulation results are provided to verify with the feasibility of the proposed system.

## 2. Block Diagrams

The block diagrams of the hybrid wind/solar cell energy system is shown in Figures

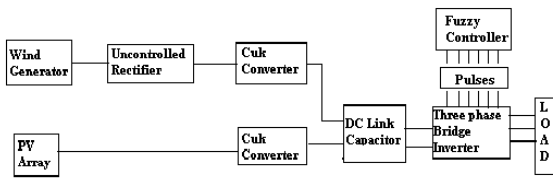


Figure 2: Block diagram of Hybrid system with multi connected cuk converter

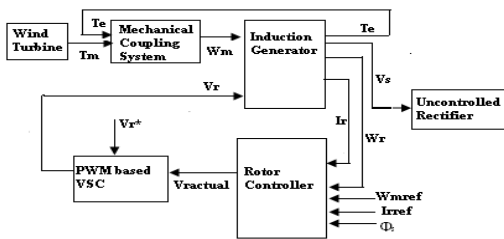


Figure 3: Block diagram of Wind Generator

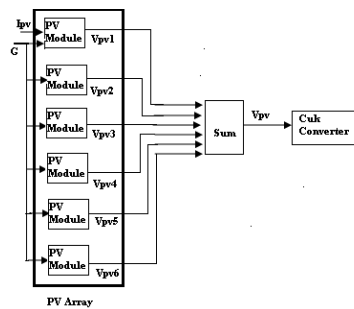


Figure 4: Block diagram of PV Array

### 2.1 Analysis of Hybrid Circuit

A system diagram of the proposed rectifier stage of a hybrid energy system is shown in Figure 2, where one of the inputs is connected to the output of the PV array and the other input connected to the output of a generator. The fusion of the two cuk converters is achieved by reconfiguring the two existing diodes from each converter and the shared utilization of the output inductor by the cuk converter. This configuration allows each converter to operate simultaneously source is available. Figure 5 illustrates the case when only the wind source is available. In this case D2 turns on, the proposed circuit becomes a cuk converter and the input to output voltage relationship is given by (1). On the other hand, if only the PV source is available, then D1 will always be on and the circuit becomes a Cuk converter as shown in Figure 6. The input to output voltage relationship is given by (2).

$$\frac{V_{dc}}{V_w} = \frac{D_2}{1-D_2} \quad (1)$$

$$\frac{V_{dc}}{V_{pv}} = \frac{D_1}{1-D_1} \quad (2)$$

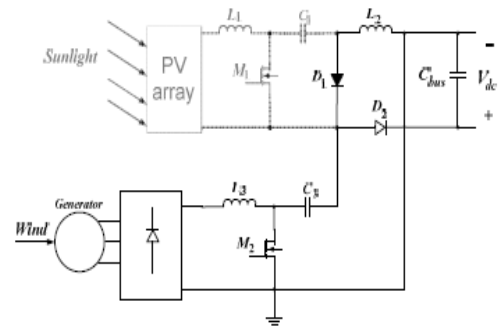


Figure 5: Only wind source is operational

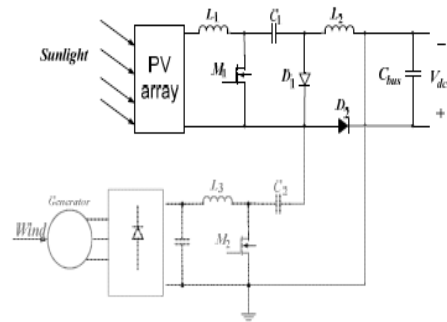


Figure 6: Only PV source is operational

To find an expression for the output DC bus voltage,  $V_{dc}$ , the volt-balance of the output inductor,  $L_2$ , is examined according to Figure 7 with  $D_2 > D_1$ . Since the net change in the voltage of  $L_2$  is zero, applying volt-balance to  $L_2$  results in (3).

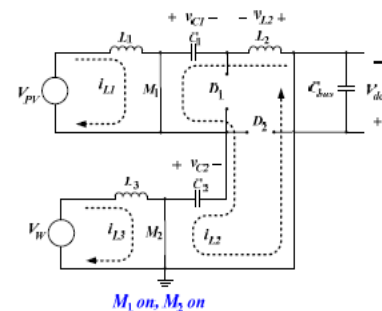


Figure 7: Rectifier stage for a Hybrid wind/PV system

The expression that relates the average output DC voltage ( $V_{dc}$ ) to the capacitor voltages ( $v_{c1}$  and  $v_{c2}$ ) is then obtained as shown in (4), where  $v_{c1}$  and  $v_{c2}$  can then be obtained by applying volt-balance to  $L_1$  and  $L_3$ . The final expression that relates the average output voltage and the three input sources ( $V_w$ ,  $V_{pv}$ ) is then given by (4). It is observed that  $V_{dc}$  is simply the sum of three output voltages of the three Cuk converters. This further implies that  $V_{dc}$  can be controlled by  $D_1$  and  $D_2$  individually or simultaneously.

$$V_{dc} = \left(\frac{D_1}{1-D_1}\right) V_{C1} + \left(\frac{D_2}{1-D_2}\right) V_{C2} \quad (3)$$

$$V_{dc} = \left(\frac{D_1}{1-D_1}\right)V_{pv} + \left(\frac{D_2}{1-D_2}\right)V_w \quad (4)$$

The switches voltage and current characteristics are also provided in this section. The voltage stress is given by (5) and (6) respectively. As for the current stress, it is observed from Figure 7 that the peak current always occurs at the end of the on-time of the MOSFET. All the Cuk Converters have MOSFET current consists of both the input current and the capacitors (C1 or C2) current. The peak current stress of M1 and M2 are given by (7) and (9) respectively. Leq1 and Leq2 given by (8) and (10) represent the equivalent inductance of three Cuk converters respectively. The PV output current, which is also equal to the average input current of the Cuk converter, is given in (11). It can be observed that the average inductor current is a function of its respective duty cycle (D1). Therefore by adjusting the respective duty cycles for each energy source, maximum power point tracking can be achieved.

$$V_{ds1} = V_{pv} \left(1 + \frac{D_1}{1-D_1}\right) \quad (5)$$

$$V_{ds2} = V_w \left(1 + \frac{D_2}{1-D_2}\right) \quad (6)$$

$$I_{ds1,pk} = I_{i,pv} + I_{dc,avg} + \frac{V_{pv} D_1 T_s}{2L_{eq1}} \quad (7)$$

$$L_{eq1} = \frac{L_1 L_2}{L_1 + L_2} \quad (8)$$

$$I_{ds2,pk} = I_{i,w} + I_{dc,avg} + \frac{V_w D_2 T_s}{2L_{eq2}} \quad (9)$$

$$L_{eq2} = \frac{L_3 L_4}{L_3 + L_4} \quad (10)$$

$$I_{i,pv} = \frac{P_G}{V_{ds1}} \left(\frac{D_1}{1-D_1}\right) \quad (11)$$

### 3. MPPT Control of Hybrid System Circuit

A common inherent drawback of wind, PV cell systems is the intermittent nature of their energy sources. Wind energy is capable of supplying large amounts of power but its presence is highly unpredictable as it can be here one moment and gone in another. Solar energy is present throughout the day, but the solar irradiation levels vary due to sun intensity and unpredictable shadows cast by clouds, birds, trees, etc. These drawbacks tend to make these renewable systems inefficient. However, by incorporating maximum power point tracking (MPPT) algorithms, the systems' power transfer efficiency can be improved significantly. To describe a wind turbine's power characteristic, equation (12) describes the mechanical power that is generated by the wind.

$$P_m = (1/2)\rho A C_p v^3 \quad (12)$$

$\rho$  = Air density (Kg/m<sup>3</sup>)

A = Swept area (m<sup>2</sup>)

C<sub>p</sub> = Power coefficient of the wind turbine

V = Wind speed (m/s)

The power coefficient (C<sub>p</sub>) is a nonlinear function that represents the efficiency of the wind turbine to convert wind energy into mechanical energy. It is dependent on

two variables, the tip speed ratio (TSR) and the pitch angle. The TSR,  $\lambda$ , refers to a ratio of the turbine angular speed over the wind speed. The mathematical representation of the TSR is given by (13).

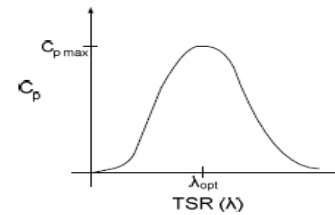


Figure 8: Power Coefficient Curve for a typical wind turbine

The pitch angle,  $\beta$ , refers to the angle in which the turbine blades are aligned with respect to its longitudinal axis.

$$\lambda = (\omega R) / v \quad (13)$$

Where

R = turbine radius,

$\omega b$  = angular rotational speed

Figure 8 and 9 are illustrations of a power coefficient curve and power curve for a typical fixed pitch ( $\beta = 0$ ) horizontal axis wind turbine. It can be seen from figure 8 and 9 that the power curves for each wind speed has a shape similar to that of the power coefficient curve. Because the TSR is a ratio between the turbine rotational speed and the wind speed, it follows that each wind speed would have a different corresponding optimal rotational speed that gives the optimal TSR.

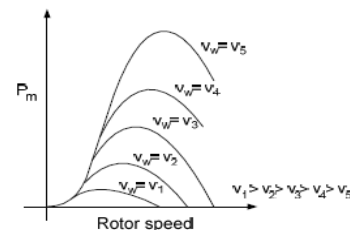


Figure 9: Power Curves for a typical wind turbine

For each turbine there is an optimal TSR value that corresponds to a maximum value of the power coefficient (C<sub>p</sub>, max) and therefore the maximum power. Therefore by controlling rotational speed, (by means of adjusting the electrical loading of the turbine generator) maximum power can be obtained for different wind speeds. A solar cell is comprised of a P-N junction semiconductor that produces currents via the photovoltaic effect.

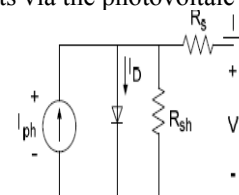


Figure 10: PV cell equivalent circuit

PV arrays are constructed by placing numerous solar cells connected in series and in parallel. A PV cell is a diode of

a large-area forward bias with a photo voltage and the equivalent circuit is shown by Figure 10. The current-voltage characteristic of a solar cell is derived in as follows:

$$I = I_{ph} - I_D \tag{14}$$

$$I = I_{ph} - I_0 \exp \left[ \frac{q(V + I R_s)}{A k_B T} - 1 \right] - \frac{V + I R_s}{R_{sh}} \tag{15}$$

Where

- I<sub>ph</sub> = photocurrent,
- I<sub>D</sub> = diode current,
- I<sub>0</sub> = saturation current,
- A = ideality factor,
- q = electronic charge 1.6x10<sup>-19</sup>,
- k<sub>B</sub> = Boltzmann's gas constant (1.38x10<sup>-23</sup>),
- T = cell temperature,
- R<sub>s</sub> = series resistance,
- R<sub>sh</sub> = shunt resistance,
- I = cell current,
- V = cell voltage.

Typically, the shunt resistance (R<sub>sh</sub>) is very large and the series resistance (R<sub>s</sub>) is very small. Therefore, it is common to neglect these resistances in order to simplify the solar cell model. The resultant ideal voltage-current characteristic of a photovoltaic cell is given by (16) and illustrated by Figure 11.

$$I = I_{ph} - I_0 \left[ \exp \left( \frac{qV}{k_B T} \right) - 1 \right] \tag{16}$$

The typical output power characteristics of a PV array under various degrees of irradiation is illustrated by Figure 12. It can be observed in Figure 12 that there is a particular optimal voltage for each irradiation level that corresponds to maximum output power.

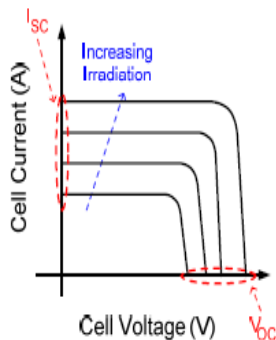


Figure 11: PV cell voltage-current characteristic

Therefore by adjusting the output current (or voltage) of the PV array, maximum power from the array can be drawn. Due to the similarities of the shape of the wind and PV array power curves, a similar maximum power point tracking scheme known the standard perturb and observe method is often applied to these energy sources to extract maximum power.

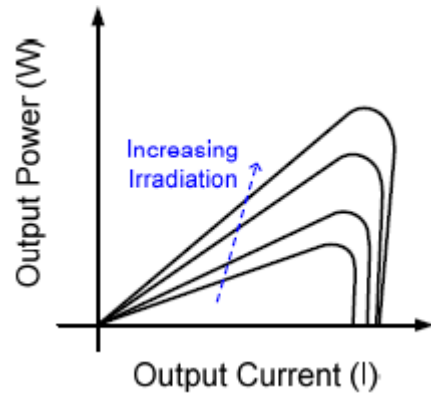


Figure 12: PV cell power characteristics

The standard perturbs and observes method for the PV system. This perturbs the operating point of the system and observes the output. If the direction of the perturbation (e.g an increase or decrease in the output voltage of a PV array) results in a positive change in the output power, then the control algorithm will continue in the direction of the previous perturbation. Conversely, if a negative change in the output power is observed, then the control algorithm will reverse the direction of the pervious perturbation step. In the case that the change in power is close to zero (within a specified range) then the algorithm will invoke no changes to the system operating point since it corresponds to the maximum power point (the peak of the power curves). Figure 13 is the flow chart that illustrates the implemented MPPT scheme.

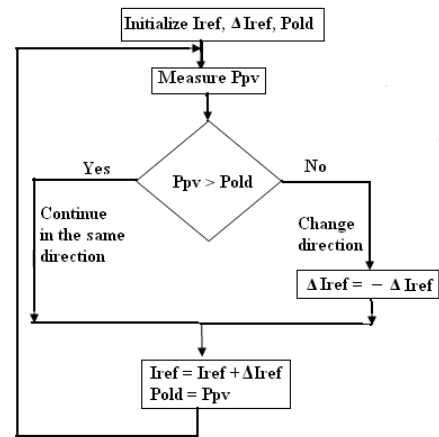


Figure 13: General MPPT Flow Chart for PV

#### 4. MATLAB / SIMULINK Model for Hybrid System

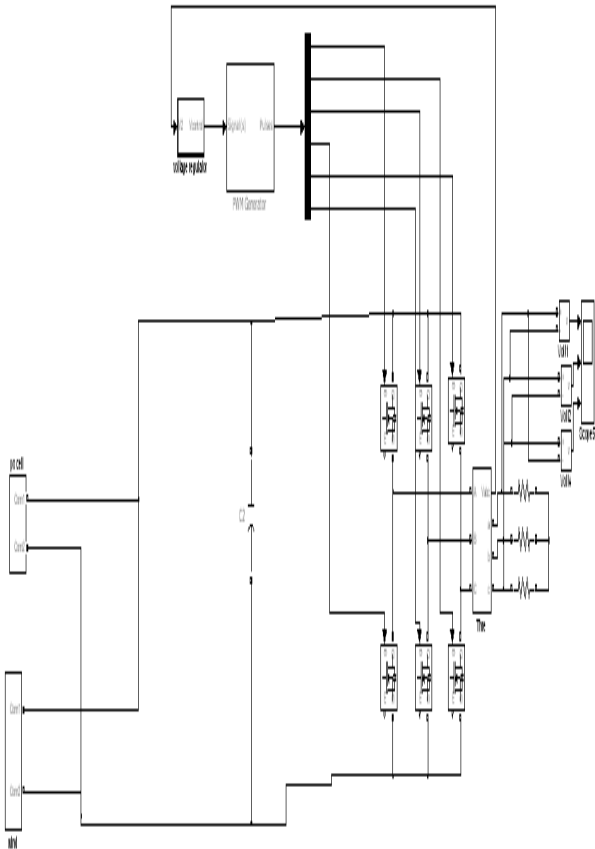


Figure 14: Simulink model for Hybrid wind/solar system

#### 5. Results and Discussions

The simulated results of the proposed multi-input rectifier stage are presented below and they can support individual as well as simultaneous operation

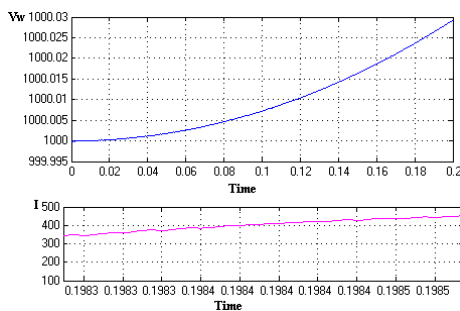


Figure 15: Individual operation with only Wind source, Top: Output voltage, Bottom: Output currents

Figure 15 illustrates the system under condition where the PV source is failed, only wind is supplying power to the load.

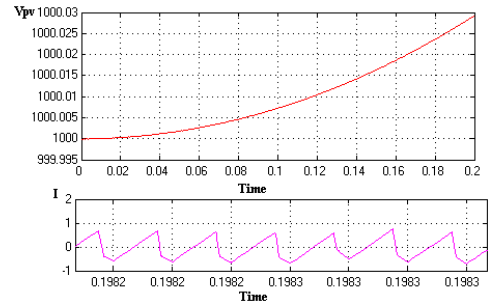


Figure 16: Individual operation with only PV source, Top: Output voltage, Bottom: Output currents

Figure 16 illustrates the system under condition where the wind source is failed, only PV is supplying power to the load

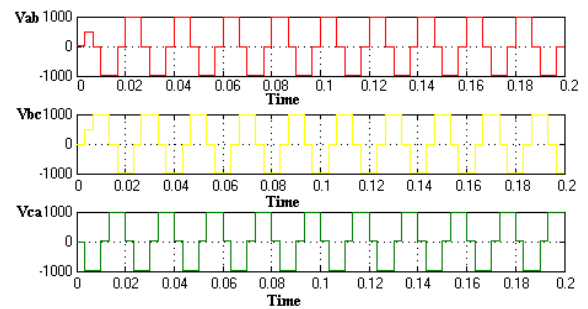


Figure 17: Output voltage across load when all the two, Sources wind/PV are in operation

Figure 17 illustrates the system output voltage of the inverter under condition where all the PV and wind sources are supplying power to the load.

#### 6. Conclusion

In the paper a novel multi-input inverter for the grid-connected hybrid Wind-PV energy system is modeled. A load demand is met by integrating of PV array and wind turbine. An inverter is used to convert output from solar & wind systems into AC power output. This system delivers power from the PV array and the wind turbine to the utility grid individually or simultaneously. Maximum power point tracking (MPPT) feature is realized for PV by standard perturbation and observation method. A large range of input voltage variation caused by different insolation and wind speed are acceptable. The firing pulses to the inverter are given by implementing Fuzzy Controller in the Hybrid Wind/PV system. This paper presents the Simulation results of various dynamic characteristics of the hybrid wind-PV system control scheme, which enables comprehensive quantitative and qualitative analysis.

#### References

- [1] Bin Lu , Yaoyu Li, Xin Wu and Zhongzhou Yang “A Review of Recent Advances in Wind Turbine Condition Monitoring and Fault Diagnosis”
- [2] Hector A. Pulgar-Painemal, Peter W. Sauer” DOUBLY-FED INDUCTION MACHINE IN WIND POWER GENERATION”

- [3] D.Aouzellag , K.Ghedamsi, E.M.Berkouk” Power Control of a Variable Speed Wind Turbine Driving an DFIG”
- [4] Kenneth E. Okedu “Stability Enhancement of DFIG-based Variable Speed Wind Turbine with a Crowbar by FACTS Device as Per Grid Requirement” INTERNATIONAL JOURNAL of RENEWABLE ENERGY RESEARCH Kenneth E. Okedu, Vol.2, No.3, 2012
- [5] B.R.Sanjeeva Reddy, Praveen Jambholkar, P.Badari Narayana, Prof. K. Srinivasa Reddy ”MPPT Algorithm Implementation for Solar Photovoltaic module using microcontroller”
- [6] Lixin Pang, Hui Wang, Yuxia Li, Jian Wang, Ziyu Wang “Analysis of Photovoltaic Charging System Based on MPPT”
- [7] Chih-Chiang Hua, Pi-Kuang Ku “Implementation of a Stand-Alone Photovoltaic Lighting System with MPPT, Battery Charger and High Brightness LEDs”
- [8] Xiaolei WANG, Pan Y AN, Liang YANG “An Engineering Design Model of Multi-cell Series-parallel Photovoltaic Array and MPPT Control” Proceedings of the 2010 International Conference on Modeling, Identification and Control, Okayama, Japan, July 17-19, 2010
- [9] F.S.Dos Reis ,J.Sebastain "characterization of Conducted Noise Generation for sepic,cuk and BoostConverters Working as Power Factor pre-regulators.”
- [10] Domingos Savio Lyrio Simonetti , Javier Sebastian “The Discontinuous Conduction Mode SEPIC and CUK Power Factor Pre-regulators: Analysis and Design” IEEE TRANSACTIONS ON INDUSTRIAL ELECTRONICS, VOL. 44, NO. 5, OCTOBER 1997
- [11] Y.-M. Chen, S.-C Hung, (2.4.C heng, and Y.-CL.i u “Multi-Input Inverter for Grid-Connected Hybrid PV/Wind Power System”